Int. J. Mach. Tool Des. Res. Vol. 23. No. 4. pp. 245–261. 1983.
Printed in Great Britain

0020–7357/83$3.00+ .00
Pergamon Press Ltd.

THE ROLE OF DISCRETE CONTACT AT THE FLANK WEAR LAND IN DETERMINING CUTTING TOOL TEMPERATURE IN ORTHOGONAL CUTTING

P. K. VENUVINOD*, W. S. LAU* and C. RUBENSTEIN*

(*Received* 10 *December* 1982; *in final form* 5 *July* 1983)

Abstract—It is shown that the assumption of continuous contact at the tool–work interface in metal cutting, as used in earlier analyses, leads to results in conflict with empirical evidence. A new model based on discrete contact at the tool flank and the associated thermal constriction resistances has been developed, from which a representative value of the flank temperature can be calculated for different cutting conditions. A relation between flank temperature and flank wear is then developed using the same discrete flank contact idealisation. The resulting flank temperature–tool life relationship is found to be of the same form as the Schallbroch–Schaumann equation. Deductions based on the assumption of discrete contact at the flank land/workpiece interface are shown to be completely consistent with experimental observation.

NOMENCLATURE

a	mean contact spot radius
A_f, A_{rf}	apparent and real contact areas at the flank respectively
c_w	volume specific heat of work material
C_n	tool–chip contact length
f_c,f_v	reduced components of F_c and F_v respectively
F	friction force at tool–chip interface
F_c,F_v	cutting force components in the direction of cutting speed and along the normal to the machined surface respectively
$(F_c)_u$, $(F_v)_u$	magnitudes of F_c and F_v for an unworn tool
F_f	friction force at tool flank
$(h_m)_o$, $(h_m)_s$, $(h_m)_f$, H_o, H	workpiece surface hardness parameters as described in the text
H_t	hardness of the surface layers of the tool flank land
H_w	mean surface hardness of work material at flank
i	index of source element at rake
i'	index of sub-area at rake
$I(i',i)$	chip-side influence coefficient relating source i and sub-area i'
j	index of source-element at flank
j'	index of sub-area at flank
J	mechanical equivalent of heat
$J(i',i)$	tool-side influence coefficient relating source i and sub-area i'
k_t, k_w	thermal conductivities of the tool and workpiece materials
$K(j',j)$	workpiece-side influence coefficient relating source j and sub-area j' when continuous flank contact is assumed
ℓ_o	magnitude of ℓ_f at the end of tool life
ℓ_f	length of flank wear land
$(\ell_f)_{cr}$	magnitude of ℓ_f at the onset of tool "burn-out"
$L(i',j)$	influence coefficient relating source j and sub-area i'
m	number of sub-areas at tool–chip interface
m'	number of sub-areas within sticking zone on rake surface
$M(j',i)$	influence coefficient relating source j' and sub-area i
n	reciprocal of index of speed in tool life equation
n'	number of sub-areas at tool–work interface
n_2	reciprocal of index of feed in tool life equation
n_3	reciprocal of index of width of cut in tool life equation
N	number of contact spots at tool–work interface
$\bar{N}$	mean spot density at tool work interface
N_f	normal load on flank land area
$N(j',j)$	tool-side influence coefficient relating source j' and sub-area j
p	probability of a tool wear particle being formed per asperity encounter
p_m	apparent normal pressure at flank land area
q	index of cutting temperature in a Schallbroch–Schaumann equation

*Department of Production & Industrial Engineering, Hong Kong Polytechnic, Hung Hom, Kowloon, Hong Kong.

MTDR 23:4–E

q'	index of $\bar{\theta}_{fs}$ in equation relating T and $\bar{\theta}_{fs}$
$q_{c,i}$	mean heat per unit area entering chip at source i
q_f	mean heat per unit area generated at apparent flank land area
q'_f	mean heat flux per unit area generated at flank contact spots
$q_{f,j}$	heat flux per unit area generated at flank source j
q_r	mean heat flux per unit area generated at tool–chip interface
$q_{r,i}$	heat flux per unit area generated at rake source i
$q_{t,i}$	heat flux per unit area entering tool at rake source i
$q_{t,j}$	heat flux per unit area entering tool at flank source j
$q_{w,j}$	heat flux per unit area entering workpiece at flank source j
r_t	unit thermal constriction resistance on tool-side at flank
$r_{t,j'}$	value of r_t at sub-area j'
r_w	unit thermal constriction resistance on workpiece-side at flank
$r_{w,j'}$	value of r_w at sub-area j'
R_f	partition coefficient (fraction of heat flux entering tool) at flank
$\bar{R}_f$	mean value of R_f
$\bar{R}_r$	mean partition coefficient (fraction of heat flux entering tool) at rake surface
t	time
t_1	uncut chip thickness
$\bar{t}(V)$	mean contact time of contact spots at flank
T	tool life
V	cutting speed
V_c	chip speed
W	length of cutting edge in engagement
Y	yield stress of work material
z	volume wear at tool flank
z_v	non-dimensional contact time parameter
α_n	tool rake angle
β_n	tool clearance angle
γ	index of W in equation for $\bar{\theta}_{fs}$
δ	index of ℓ_f in equation for $\bar{\theta}_{fs}$
ω	a parameter related to the nature of adhesion wear
ϵ	index of V in equation for $\bar{\theta}_{fs}$
η	index of t_1 in equation for $\bar{\theta}_{fs}$
η'	ratio $\Delta\bar{\theta}/\Delta\bar{\theta}_\infty$
ζ	a non-dimensional parameter
ζ_a	chip thickness ratio
θ_o	ambient temperature
$\theta_{c,i'}$	temperature at sub-area i' calculated from the chip-side
$\Delta\theta_{c,i'}$	temperature rise at sub-area i' calculated from the chip-side
θ_f	representative flank wear land temperature
$\bar{\theta}_f$	mean flank temperature assuming smooth contact at flank
$\theta_{fs,j'}$	mean spot temperature at sub-area j'
$\bar{\theta}_{fs}$	mean spot temperature at flank
$\theta_{fst,j'}$	mean spot temperature at sub-area j' calculated from tool side
$\theta_{r,i'}$	mean temperature at sub-area i'
$\theta_{fsw,j'}$	mean spot temperature at sub-area j' calculated from workpiece side
θ_m	tool-work thermocouple temperature
$\bar{\theta}_r$	mean temperature at tool–chip interface
$\bar{\theta}_s$	mean shear plane temperature
$\theta_{t,i'}$, $\theta_{t,j'}$	temperatures at sub-areas i' and j' respectively calculated from tool side
$\theta_{w,i'}$	temperature at sub-area i' calculated from workpiece side
$\Delta\bar{\theta}$	mean temperature rise of a contact spot at finite contact time
$\Delta\bar{\theta}_\infty$	mean temperature rise of a contact spot at infinite time
e, K, K_1, K_2, K_f, q'', u, v	constants

INTRODUCTION

TWO MODELS have been proposed by which the temperatures at the interface between two sliding surfaces can be calculated. The first, proposed by Carslaw and Jaeger [1, 2], assumes that the contacting surfaces are perfectly smooth while the second, proposed by Holm [3, 4], recognises the fact that manufactured surfaces are never perfectly smooth and assumes that contact between sliding surfaces occurs at discrete points. Notwithstanding the fact that models formulated to explain cutting tool flank face wear have assumed that contact occurs at discrete points [5, 6], cutting tool temperatures have been calculated assuming that the tool–chip contact *and the tool–workpiece contact* are perfectly smooth—strangely, this inconsistency does not appear to have been noted previously.

If, following [7], temperatures in the flank wear land surface are computed for H.S.S. tools cutting mild steel assuming smooth tool/work contact, it is found (see below) that deductions are at variance with experimental observation. In the light of this evidence the assumption of smooth flank land/workpiece contact becomes questionable and the aim of the present work is to explore the consequences of assuming discrete contact between tool and workpiece.

THEORETICAL CONSIDERATIONS

Tool/workpiece contact

The tool and workpiece are in contact over the rake face, round the cutting edge, along the flank wear land and over a portion of the clearance face i.e. over the region TT′ODFE (Fig. 1). Much experimental evidence exists [8–13] to support the generally accepted view that over the portion OT′ the chip sticks to the rake face and the contact is continuous. In contrast, over the region TT′ the chip is believed to slide over the rake face and contact occurs at discrete spots. Although it has been assumed [7, 14, 15] that the heat generation rate is uniform over the whole of the contact region, OT, a more realistic assumption [16] is that the heat generation rate is uniform over OT′ and is linearly decreasing over TT′ and this assumption will be adopted here.

Consider, now, the contact between the tool and the workpiece. Elsewhere [17] it has been shown that a thin layer of workpiece material is extruded below the cutting edge and maintains contact with the tool over ODFE (Fig. 1). This model has been shown to account for the dependence of the cutting force components on the uncut chip thickness and explains the workpiece hardening resulting from cutting [18]. If the pressure between the workpiece and the flank wear land is p_m, the normal cutting force component, F_v, varies linearly with the flank wear land area, A_f,—the slope being p_m [17]. For mild steel cut by H.S.S. it was found, empirically, that $p_m \simeq Y/3$ where Y is the yield stress of the work material i.e. the mean stress acting over the apparent area is in the elastic range. Similar results were obtained in the experiments by Kobayashi and Thomsen [19] and in the present work. Real area is thus smaller than apparent area i.e. contact over the flank face is discrete.

Thus, while it is legitimate to assume the chip/tool contact is continuous, over the flank face contact is discrete. Notwithstanding the fact that at any instant there will be a spectrum of asperity contact sizes we will assume, for simplicity, that all contact spots are circular, equal in size and uniformly distributed (Fig. 2). This simplifying assumption is commonly introduced when models are formulated to explain the temperatures [3, 4], the friction [20] and the wear [21] of sliding surfaces and the wear of cutting tools [5]. In

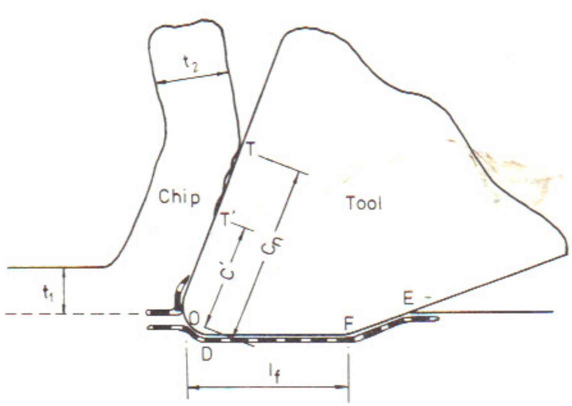

FIG. 1. Schematic diagram of tool/workpiece combination.

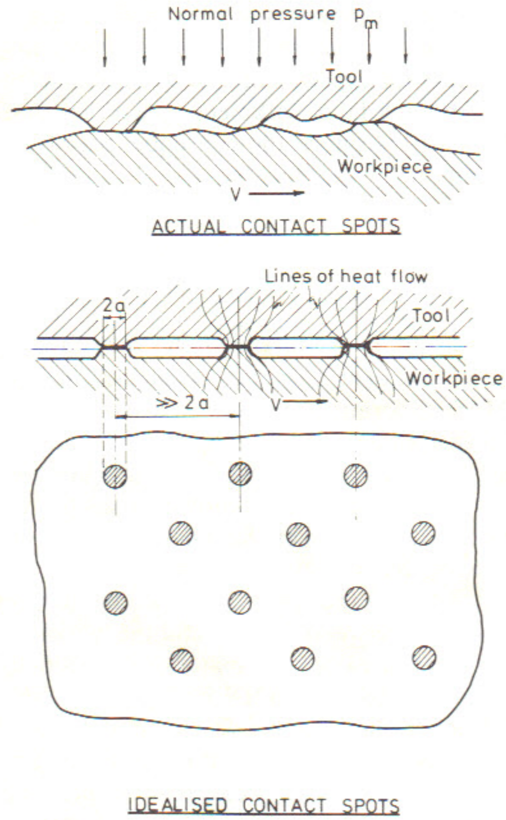

FIG. 2. The discrete nature of contact at the flank surface.

order to calculate temperatures assuming discrete flank contacts we must first determine the thermal constriction resistance at the flank contact zone.

Thermal constriction resistance at flank surface

The normal loads on FE (Fig. 1) are usually very small so that this zone can be excluded from the analysis. The measured flank wear land ℓ_f includes OD which, however, is usually very small compared to DF so that the apparent area at the tool flank may be taken as

$$A_f = W\ell_f. \tag{1}$$

Let there be N asperity contacts in this area so that the mean spot density $\bar{N}$ is given by

$$\bar{N} = N/A_f. \tag{2}$$

The real area of contact A_{rf} is given by

$$A_{rf} = \frac{p_m A_f}{H_w} \tag{3}$$

where p_m is the mean normal stress over A_f and H_w is the mean hardness of the surface layers of the workpiece.*

*It will be noted that no attempt has been made to allow for junction growth—this is because junction growth is of importance only for soft metals or for oxide-free harder metals [20, p. 359].

The radius a of the idealised contact spots is then given by

$$a = \left(\frac{A_{rf}}{\pi N}\right)^{\frac{1}{2}} = \left(\frac{p_m}{\pi \bar{N}\ H_w}\right)^{\frac{1}{2}}. \quad (4)$$

The rate of frictional heat generation per unit apparent flank area is

$$q_f = \frac{F_f V}{JW\ell_f} \quad (5)$$

where F_f is the friction force along the flank wear land, V is the cutting speed and J is the mechanical equivalent of heat.

This heat is in fact generated at the contact spots so that the mean rate of heat generation per unit true area is

$$q_f' = \frac{q_f}{\pi a^2 \bar{N}}. \quad (6)$$

A fraction R_f of this heat flux flows into the tool and the rest, i.e. $(1 - R_f)q_f'$, into the workpiece. However, these heat fluxes, generated in a small and finite area, are to be conducted into what are, effectively, semi-infinite conducting media, viz, the tool and the workpiece, so that the associated thermal constriction resistances must be introduced.

Estimation of thermal constriction resistances

The constriction resistances may be estimated by following the procedure developed by Holm [3, 4] for sliding contacts. Holm replaced the actual curved heat flow lines by straight lines radiating from a hemispherical surface of suitable radius, of finite thermal conductivity and of zero heat capacity and then derived the parameters of this model from a flat circular contact spot of radius a. Following Jaeger's approach [1, 2] the flat contact spots were then considered as a moving heat source with respect to the sliding surface (workpiece) with velocity equal to the sliding speed (V) and a stationary heat source of finite duration with respect to the slider (tool), the duration of heating in non-dimensional form being given by

$$z_v = \frac{\pi k_w}{2Vac_w}. \quad (7)$$

where k_w and c_w are the thermal conductivity and volume specific heat respectively of the sliding member (workpiece). The fraction of heat flux entering the sliding surface $(1 - R_f)$ and the steady state temperature rise, $\Delta\bar{\theta}_\infty$, were then estimated and, thereafter, the actual temperature rise $\Delta\bar{\theta}$ was defined as a fraction η' of $\Delta\bar{\theta}_\infty$ i.e.

$$\Delta\bar{\theta} = \eta'\Delta\bar{\theta}_\infty = \frac{\eta' a q_f'}{(k_w + k_t\zeta)}. \quad (8)$$

where η' and ζ are non-dimensional numbers that can be estimated from Figs 21.06 and 21.18 of reference [3] for a given z_v.

It is convenient at this stage to define unit thermal constriction resistance as the ratio of temperature rise at a contact spot to heat flux per unit apparent area. Combining equations (1)–(8), the unit thermal constriction resistances r_t and r_w on the tool and workpiece sides respectively may be expressed as

$$r_t = \frac{\Delta\bar{\theta}}{R_f q_f} = \frac{\eta'}{\pi a \bar{N} \zeta k_t}. \quad (9)$$

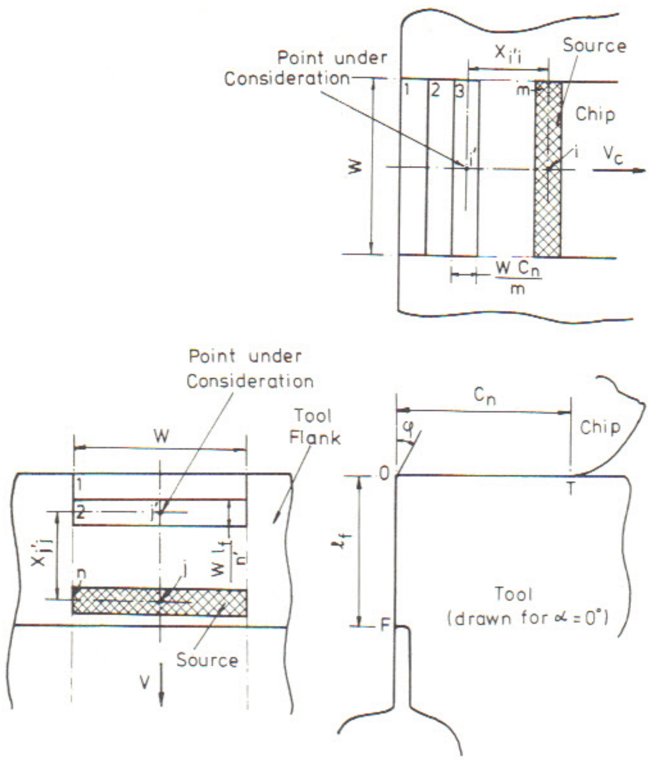

FIG. 3. Idealisation of heat sources at the tool/chip and tool/work interfaces in free orthogonal cutting.

and

$$r_w = \frac{\Delta\bar{\theta}}{(1 - R_f)q_f} = \frac{\eta'}{\pi a \bar{N} k_w}. \tag{10}$$

Estimation of temperature distributions assuming continuous contact at rake and discrete contact at flank

Figure 3 shows the idealisation adopted here to estimate the temperature distributions at the flank and rake surfaces for free orthogonal cutting. The rectangular tool–chip contact area, $W \times C_n$, is sub-divided into m contiguous rectangular band sources of dimensions $W \times C_n/m$ while the tool–work contact area, $W \times \ell_f$, is sub-divided into n' contiguous rectangular bands of dimensions $W \times \ell_f/n'$. Let $q_{r,i}$ and $q_{f,j}$ be the heat fluxes per unit apparent area liberated at band source i on the rake surface and source j at the flank surface respectively. Further, let $q_{c,i}$ and $q_{t,i}$ be the heat fluxes per unit apparent area entering the chip and the tool at source i and $q_{w,j}$ and $q_{t,j}$ be those entering the workpiece and the tool at source j. Clearly

$$q_{c,i} + q_{t,i} = q_{r,i} \text{ and } q_{w,j} + q_{t,j} = q_{f,j}. \tag{11a,b}$$

Consider now the mean spot temperature $\theta_{fs,j'}$ at band j' at the flank. Let $\theta_{fsw,j'}$ be its estimate obtained from moving heat source considerations on the workpiece side and $\theta_{fst,j'}$ be the estimate obtained from stationary heat source considerations on the tool side. Then,

$$\theta_{fsw,j'} = \theta_{fst,j'} = \theta_{fs,j'}. \tag{12}$$

Next, consider $\theta_{fsw,j'}$, which must exceed the workpiece surface temperature, immediately adjacent to the constriction spots, by the amount $q_{w,j'}\, r_{w,j'}$ where $r_{w,j'}$ is the workpiece side unit thermal constriction resistance at j' calculated from equation (10). We need not consider the heat flow between contact spots through the workpiece since Holm [3, 4] has shown that the heating and cooling times of the spots between successive encounters are of the same order which means that provided the mean inter-spot distance is large compared to the spot size (i.e. $\bar{N}$ not too large), the spots have adequate time between successive encounters to cool down to the ambient workpiece temperature (assumed to be equal to room temperature θ_o). Thus we can write

$$\begin{aligned}\bar{\theta}_{fsw,j'} &= \theta_o && \text{when } j' \neq j \text{ and}\\ &= \theta_o + q_{w,j}\, r_{w,j'} && \text{when } j' = j.\end{aligned} \tag{13}$$

Likewise $\theta_{fst,j'}$ should be higher than the temperature $\theta_{t,j'}$ in the tool material immediately adjacent to the constriction spots at band j' by $q_{t,j'} r_{t,j'}$ where $r_{t,j'}$ can be obtained using equation (9). Here $\theta_{t,j'}$ cannot be taken equal to θ_o because of the stationary nature of the heat sources with respect to the tool. In this case, there is plenty of time for the heat sources near j' to influence the temperature at j' by conduction through the tool material. Obviously, $\theta_{t,j'}$ involves the summation of the temperature rises due to the m band sources at rake (of strength $q_{t,i}$) and $(n' - 1)$ flank sources (of strengths $q_{t,j}$ for $j' \neq j$). Accordingly, we may write

$$\begin{aligned}\bar{\theta}_{fst,j'} &= \theta_o + \sum_{i=1}^{m} q_{t,i}\, M(j',i) + \sum_{j=1}^{n'} q_{t,j}\, N(j',j) \text{ (when } j' \neq j)\\ &= \theta_o + \sum_{i=1}^{m} q_{t,i}\, M(j',i) + \sum_{j=1}^{n'} q_{t,j}\, N(j',j)\\ &\quad + q_{t,j}\, r_{t,j'} \text{ (when } j' = j).\end{aligned} \tag{14}$$

where $M(j',i)$ and $N(j',j)$ are appropriate influence coefficients (an influence, say $X(a,b)$, being defined as the temperature rise at band a due to unit heat flux per unit apparent area entering the conducting material at band source b).

Consider next the temperature $\theta_{r,i'}$ at band i' on the rake face. Two estimates for this can be obtained, namely, $\theta_{c,i'}$ from moving heat source considerations on the chip side and $\theta_{t,i'}$ from stationary heat source considerations on the tool side. Since the chip/tool contact is continuous there is no constriction resistance but interactions between rake sources via thermal conduction through the chip material must be considered.

Accordingly we may write

$$\theta_{c,i'} = \bar{\theta}_s + \sum_{i=1}^{m} q_{c,i}\, I(i',i) \tag{15}$$

$$\theta_{t,i'} = \theta_o + \sum_{i=1}^{m} q_{t,i}\, J(i',i) + \sum_{j=1}^{n'} q_{t,j}\, L(i',j) \tag{16}$$

and

$$\theta_{c,i'} = \theta_{t,i'} = \theta_{r,i'} \tag{17}$$

where $I(i',i)$, $J(i',i)$, $L(i',j)$ are appropriate influence coefficients and $\bar{\theta}_s$ is the initial chip temperature assumed equal to the mean shear plane temperature.

Equations (11)–(17) can be combined and solved simultaneously to yield temperature distributions $\theta_{r,i'}$ and $\theta_{f,j'}$ at the rake and flank surfaces for any given set of initial workpiece temperature θ_o, shear plane temperature $\bar{\theta}_s$, rake and flank frictional heat flux distributions $q_{r,i}$ and $q_{f,j}$, and arrays of influence coefficients $I(i',i)$, $j(i',i)$, $L(i',j)$, $M(j',i)$ and $N(j',j)$.

In the present work θ_o is taken as 25°C and $\bar{\theta}_s$ is estimated from measured cutting force components and chip dimensions using the procedure of Loewen and Shaw [14]. Heat flux generation at the flank wear land is taken to be uniform so that $q_{f,j'} = q_f$ where q_f is given by $q_f = F_f V/JW\ell_f$ where J is the mechanical equivalent of heat. The heat flux generation $q_{r,i}$ at the tool–chip interface was estimated using the procedure detailed in [16] assuming constant heat generation rate over the sticking zone (covering m' band sources) and a linearly decreasing generation rate in the sliding zone with the total heat liberation rate at the chip–tool interface being FV_c/J where V_c is the chip speed and F is the friction force at the chip–tool interface.

The influence coefficients I (i',i), ..., $N(j',j)$ have been estimated by adopting a procedure similar to that used by Chao and Trigger [7] in their analysis of temperatures in zero rake orthogonal corner tools, for which purpose they constructed a source idealisation similar to that shown in Fig. 3. However, since their analysis was for corner tools, Chao and Trigger [7] had to create mirror images of the various band sources so that the width of each combined band source became $2W$ instead of W and the point of estimation of temperature was taken to be at a distance $W/2$ from the edge along the centre line of the band. However there is no need to construct mirror images for free orthogonal cutting so that Fig. 3 is a complete description of source idealisation in the present work. The above modifications to the Chao and Trigger analysis represent minor refinements and the resulting equations for $I(i',i)$ etc. are omitted since their inclusion here could only serve to distract attention from the physical argument.

Two further refinements to the analysis given in [7] have been introduced in the present work. These are:

1. The introduction of a numerical iterative procedure to take into account the temperature dependence of the thermal properties of the workpiece and chip materials; and
2. In estimating the magnitudes of the influence coefficients $L(i',j)$ and $M(j',i)$, the influence of rake angle on the distance between a point on the rake surface and another on the flank surface has been taken into account (whereas in [7] the rake angle was taken as zero).

Once the temperature and heat flux distributions are known the mean partition coefficients of heat flux $\bar{R}_r$ and $\bar{R}_f$ at the rake and flank contact regions, the mean rake temperature $\bar{\theta}_r$ and the mean flank spot temperature $\bar{\theta}_{fs}$ can be calculated.

Later in the paper, an attempt will be made to compare the results obtained from the assumption of discrete flank contact with those derived by assuming continuous flank contact. When the latter assumption is employed, the procedure used to estimate the temperature distributions is the same as that described above except that equations (12) and (13) are replaced by the following equations (after [7])

$$\theta_{t,j'} = \theta_{w,j'} = \theta_{f,j'} \text{ and} \tag{18}$$

$$\theta_{w,j'} = \theta_o + \sum_{j=1}^{n'} q_{t,j}\, K(j',j) \tag{19}$$

where $K(j',j)$ is the influence coefficient given by the temperature rise at j' due to unit heat flux entering the moving workpiece at j.

Thus, the mean flank temperature $\bar{\theta}_f$ obtained by assuming continuous flank contact is equal to

$$(1/n') \quad (\sum_{j=1}^{n'} \theta_{w,j'}).$$

The nature of $\bar{\theta}_{fs}$

In reality the size, shape, distribution and temperatures of the contact spots will be determined statistically. Notwithstanding the simplifications introduced with the idealised circular spot model, deductions therefrom have been found to explain wear phenomena quite well [5, 6, 21] so that although we cannot hope to attribute a definite physical meaning to $\bar{\theta}_{fs}$, we may consider it to be a representative measure of the temperature fields existing in the vicinity of the tool-work interface. This means, however, that $\bar{\theta}_{fs}$ can only be verified indirectly viz., by selecting a process known to be sensitive to θ_{fs} and comparing theoretical deduction with experimental observation. To this end, the relation between $\bar{\theta}_{fs}$ and the flank wear of cutting tools is now explored.

The relationship between $\bar{\theta}_{fs}$ *and tool wear*

Schallbroch and Schaumann [22] identified the relationship between cutting temperature and tool life T in their equation

$$T\,\theta_m{}^q = \text{constant} \tag{20}$$

where q is a constant for a given tool–workpiece combination.

However, when tool life is determined by a flank wear land criterion, T should be a function of the mean wear land temperature, θ_f. Assuming that flank wear occurs exclusively by the adhesion mechanism due to weld formation at asperity junctions, it has been shown recently [5] that

$$T\,\theta_f{}^{q'} = \text{constant} \tag{21}$$

where q' is a constant for a given tool–work combination.

The effect of cutting conditions on tool life T can be expressed as

$$T = \frac{\text{constant}}{V^{1/n_1} t_1^{1/n_2} \ell^{1/n_3}}\,. \tag{22}$$

Following [6] let it be assumed that $\bar{\theta}_{fs}$ can be expressed in the form

$$\bar{\theta}_{fs} = K\,V^{\epsilon}\,t_1{}^{\eta}\,W^{\gamma}\,\ell^{\delta}{}_f \tag{23}$$

where K is a constant.

With a view to establishing the significance of $\bar{\theta}_{fs}$, the relationship between the indices appearing in equation (22) and those in equation (23) will now be determined following the procedure adopted in [5].

In accordance with proposals originally advanced by Holm [3] and later modified by Burwell and Strang [23], there is a probability, p_w, that the rupture of a tool/workpiece junction will produce a workpiece wear particle and a probability, p, that a tool wear particle will be produced. Since we are only interested in tool wear, the magnitude of p_w is immaterial and following a procedure similar to that given in [6] it can be shown that the volume wear rate at the tool flank is

$$\frac{dz}{dt} = K_1\,\bar{\theta}_{fs}{}^{q''}\,N_f{}^{\omega} = K_1\,\bar{\theta}_{fs}{}^{q''}\,(p_m W \ell_f)^{\omega} \tag{24}$$

where K_1 and q'' are constants; N_f is the normal load on the tool flank-land area and ω is a constant varying from 0.75 to 1 depending on whether the wear is "layer" type or "lump" type (as distinguished by Archard [21]). The constant K_1 is proportional to the probability p which will depend, *inter alia*, on the strength (hardness, H_t) of the surface layers of the tool flank wear land. In fact p will be an inverse function of H_t which we can represent as $p \propto (H_t)^{-u}$. However, H_t will, itself, be an inverse function of the interface temperature $\bar{\theta}_{fs}$ so that if $H_t \propto (\bar{\theta}_{fs})^{-v}$ we can write $p \propto (\bar{\theta}_{fs})^{uv}$ which means that we can express K_1 as

$$K_1 = K_2(\bar{\theta}_{fs})^e \tag{25}$$

where, for a given tool/workpiece combination, K_2, e are constants.

It has been shown in [5, 6] that dz/dt is related to the rake angle α_n and clearance angle β_n as

$$\frac{dz}{dt} = \frac{W\ell_f}{(\cot\beta_n - \tan\alpha_n)}\frac{d\ell_f}{dt}. \tag{26}$$

Combining equations (24), (25) and (26)

$$\frac{d\ell_f}{dt} = K_2K^{q'}(\cot\beta_n - \tan\alpha_n)p_m{}^{\omega}V^{\epsilon q'}\,t_1{}^{\eta q'}\,W^{\gamma q'+\omega-1}\,\ell_f{}^{\delta q'+\omega-1} \tag{27}$$

where $q' = q'' + e$.

Usually, the gradual wear region, which is described by equation (27), is concave towards the wear land axis. This means that in this region $\delta q'+\omega-1 \leq 0$. It is customary, however, to represent this as a linear variation, so that

$$\delta q' + \omega - 1 \simeq 0$$

and, since $\omega = 0.75$ to 1, this gives $0 \leq q'\delta \leq 0.25$ (28)

Assuming that tool life T is obtained when the wear land ℓ_f reaches a prescribed value ℓ_o, we can integrate equation (27) in the range $\ell_f = 0$ to ℓ_o and $t = 0$ to T, in order to find T. The resulting equation can be rearranged as

$$T(\bar{\theta}_{fs})^{q'} = \text{constant}. \tag{29}$$

Combining equations (23) and (29) and equating to equation (22)

$$n\epsilon = n_2\eta = 1/q'. \tag{30}$$

Expression (28) and equations (29) and (30) will be used to verify the computed $\bar{\theta}_{fs}$.

EXPERIMENTAL DETAILS

Cutting tests were performed on a Colchester Triumph 2000 lathe using MTM 41 H.S.S. (RC65) cutting tool bits with 10° rake angle, 5° clearance angle and an obliquity of 0°. Tubular mild steel workpiece (OD 50.8 mm, wall thickness 2 mm, BHN 120) were cut at different speeds (25–55 m/min) and feeds (0.05–0.2 mm/rev). The speed range selected was high to avoid built up edge and to enable quick tool wear results. Cutting tests were interrupted at regular intervals and the flank wear land ℓ_f was measured using a tool-maker's microscope. Tool wear curves (ℓ_f–time) were plotted so that a flank wear land criterion (ℓ_o), which could result in the highest possible tool lives without any of the tools used burning out, could be selected; in this way, $\ell_o = 0.18$ mm was chosen. Cutting tests were performed both with nominally sharp tools ($\ell_f = 0$) and tools on which flank wear lands had been deliberately imposed. These lands were obtained by reversing the rotation of the workpiece and maintaining light contact between the tool and the workpiece until a predetermined land was obtained.

Cutting forces (F_v and F_c) were measured using a Kistler three-component measuring platform the outputs from which were led to a UV recorder. Cutting temperatures were measured using the tool–work thermocouple method. The tools were 150 mm long and leads to a digital voltmeter were connected to the far ends of the tools which were cooled by an air jet so as to avoid errors due to parasitic emfs. For each tool, the calibration of the tool–work thermocouples was effected using the silver bead technique. Shallow axial slots were made on the workpiece surface so that chip lengths corresponding to one revolution of the workpiece could be obtained and mean chip thickness ratios were calculated from the chip lengths. Chip–tool contact lengths were estimated by viewing the scratch patterns on the rake face through a microscope.

RESULTS AND DISCUSSION

Empirically, it was found that the cutting force components, F_c and F_v, each varied linearly with the wear land ℓ_f. From the slope of the F_v vs ℓ_f line the value of the normal stress acting on the wear land, p_m, is found to be ca 123 MPa i.e. about ⅓ of the yield stress of the workpiece material which implies that the contact at the tool/work interface is not continuous. This agrees with observations made elsewhere [5, 6].

To compute temperatures, cutting data are required. The force intercepts of the F_c vs ℓ_f and the F_v vs ℓ_f lines give the cutting force components $(F_c)_u$ and $(F_v)_u$ for an unworn tool. The friction and normal forces at the tool flank, F_f and N_f, are given by $F_f = F_c - (F_c)_u$ and $N_f = F_v - (F_v)_u$. For the present experiments this gives a coefficient of friction of 1.25 at the tool flank, which is in agreement with [17]. Neglecting the contribution resulting from cutting edge curvature, then, approximately, the reduced cutting forces (forces directly associated with chip formation) are equal to the force intercepts so that $f_c \approx (F_c)_u$ and $f_v \approx (F_v)_u$. Further, it was found experimentally that $\zeta_a = 4.8$ and $C_n = 0.81$mm at $V = 41$ m/min, $t = 0.1$ mm and $\ell_f = 0.18$ mm. Experiments at other cutting speeds and flank wear lands showed that there was no systematic variation in $(F_c)_u$, $(F_v)_u$, ζ_a and C_n. Observations at different uncut chip thicknesses showed that ζ_a remained constant whereas $(F_c)_u$, $(F_v)_u$ and C_n increased in proportion to t_1.

From the empirical variation of tool life T with cutting speed for $\ell_o = 0.18$ mm, a value of $n = 0.22$ was estimated and from the relation between tool life and uncut chip thickness a value of $n_2 = 0.86$ was obtained.

A computer programme was developed to estimate the temperature distributions. The programme used equations given in [7] which had been modified as described above to convert given sets of F_c, F_v, ζ_a, C_n, W, ℓ_f and F_f into mean heat fluxes q_r and q_f at the tool–chip interface and tool work interface respectively.

Using the thermal properties of mild steel quoted in [14] and adopting an iteration procedure so as to allow for the temperature dependence of the workpiece properties, calculations of the mean chip/tool interface temperature, $\bar{\theta}_r$, and the mean flank temperature, $\bar{\theta}_f$, were made, in the first instance, by assuming continuous contact over the tool/workpiece contact region. As might have been anticipated, the trends agreed with those given in [7] but the results were in conflict with experimental observation.

First, if we assume that $\bar{\theta}_f$ can be expressed as

$$\bar{\theta}_f = K_f\, V^{\epsilon}\, t_1^{\,\eta}\, \ell_f^{\,\delta}$$

then ϵ is found to be 0.4 while η is much smaller than would be expected viz., $\eta = 0.0047$, (Figs 4a and 4b).

Hence $\eta/\epsilon = 0.012$ whereas, equation (30) requires that

$$\frac{\eta}{\epsilon} = \frac{n}{n_2} = \frac{0.22}{0.86} = 0.26.$$

Thus, the assumption of continuous flank contact fails to predict the correct η/ϵ ratio.

Second, the dependence of $\bar{\theta}_f$ on ℓ_f yields a value $\delta = 0.41$ (Fig. 4c) and when this is substituted into expression (28) we find $0 \leqslant q' \leqslant 0.6$ which implies an extremely weak relation between tool life and flank temperature when, intuitively, a stronger relation would be anticipated.

Third, the general level of the computed $\bar{\theta}_f$ appears to be too low. It is known that H.S.S. tools "burn out" due to irreversible metallurgical transformations when they are subjected to temperatures beyond about 600°C. At $V = 41$ m/min and $t_1 = 0.1$ mm, the computed flank temperature is 310°C, even when ℓ_f is 1.6 mm. However, experiments by the authors, at these cutting conditions, showed that the tool started "burning out" when

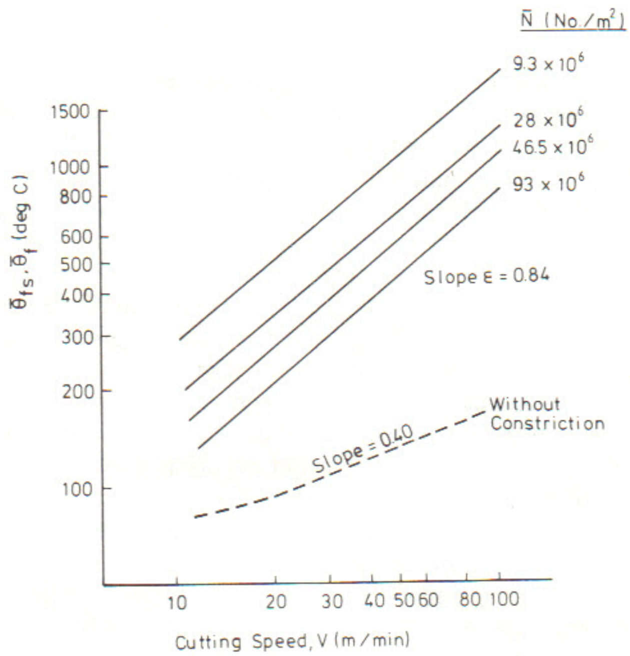

FIG. 4(a).

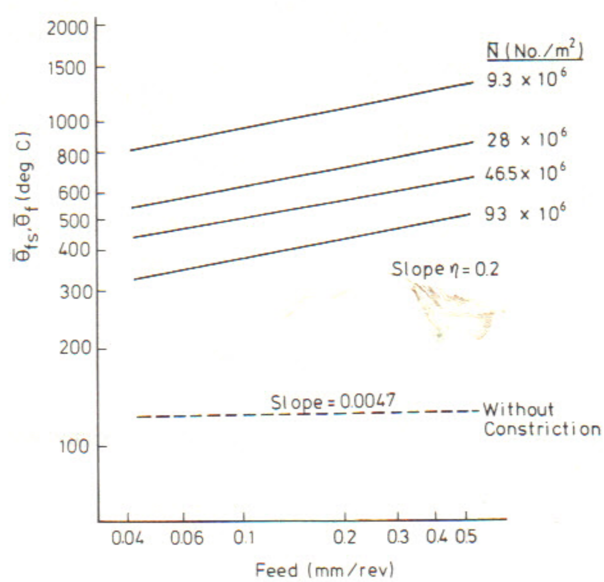

FIG. 4(b).

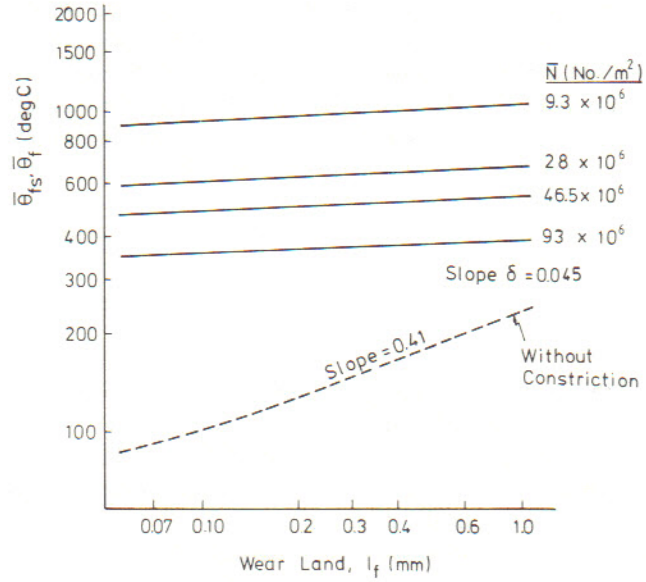

FIG. 4(c).

FIG. 4.(a) The relationship between cutting speed and the computed values of $\bar{\theta}_{fs}$ *and* $\bar{\theta}_f$ for t_1 = 0.1 mm and $\ell_f = 0.18$ mm. (b) The relationship between feed and the computed values of $\bar{\theta}_{fs}$ *and* $\bar{\theta}_f$ for $V = 41$ m/min and $\ell_f = 0.18$ mm. (c) The relationship between the length of flank wear land and the computed values of $\bar{\theta}_{fs}$ and $\bar{\theta}_f$ for V = 25–55 m/min and t_1 = 0.05–0.2 mm.

$\ell_f \simeq 1.6$ mm. Hardness surveys on the resulting "burnt" tools indicated (by comparing them to the known temperature–hardness curves of the tool material) that the temperatures in the vicinity of the flank land area had exceeded 600°C. Further, the "burnt" tools showed little thermal degradation in the vicinity of the rake surface indicating the flank to have been hotter than the rake. For H.S.S. cutting mild steel, the computed values of $\bar{\theta}_f$ and $\bar{\theta}_r$, however, suggest exactly the opposite i.e. the rake is always hotter than the flank.

Last, the maximum flank temperature does not occur within the flank land area, but at a location beyond it on the free clearance surface. It may be noted that Murarka *et al.* [15] report similar results in their finite element analysis assuming continuous contact at the tool–work interface. It is evident, however, that these results are absurd since experiments on burnt tools suggest that "burn out" occurs in the vicinity of the flank land area and not on the free clearance surface.

It will be shown now that the use of $\bar{\theta}_{fs}$ in place of $\bar{\theta}_f$ avoids all of these anomalies. However, in order to compute $\bar{\theta}_{fs}$ we need the radius of the idealised contact spot, a, and, therefore, estimates of the idealised spot density $\bar{N}$ and of the surface hardness of the workpiece H_w. In fact we have no way of obtaining an accurate estimate of $\bar{N}$ (although as we will see, it is possible to get some idea of the order of $\bar{N}$). Instead, values of $\bar{\theta}_{fs}$ have been computed using different arbitrarily chosen values for $\bar{N}$ and, as will be seen, it turns out that the important parameters are insensitive to the actual value $\bar{N}$ so that our lack of an accurate estimate is of little import. Concerning H_w, it is known [18] that the work surface is considerably work-hardened by the time it approaches the flank land area. The depth of the work-hardened layer is usually quite large compared to the likely size of flank contact spots. Consequently, it is reasonable to take H_w, in equation (4) as the mean surface hardness of the workpiece at the flank land area. In [18] it was shown empirically that the hardness of the machined surface is given by

$$H = H_o + (h_m)_o + (h_m)_s + (h_m)_f$$

where H_o is the initial workpiece hardness, and $(h_m)_o$, $(h_m)_s$ and $(h_m)_f$ are the increases in surface hardness due to extrusion under the cutting edge, while traversing the primary deformation zone and while traversing the flank land respectively.

For mild steel, it is found that [18] $H_o = 122.4$ kg/mm^2, $(h_m)_o = 40.8$ kg/mm^2, $(h_m)_s = 79\, t_2 \sec \alpha_n$ kg/mm^2 and $(h_m)_f = 23.6\, \ell_f$ kg/mm^2, where t_2 and ℓ_f are in mm.

Taking H_w to be equal to the mean surface hardness of the work material under the flank land area

$$H_w = 163.2 + 79\, t_2 \sec\alpha_n + 23.6\, \frac{\ell_f}{2}. \tag{31}$$

It will be assumed that equation (31) may be applied in the entire range of cutting speeds and feeds used. Knowing H_w and $\bar{N}$, it is now possible to determine the spot radius, a, for given values of p_m and by following the procedures described above, values of $\bar{\theta}_{fs}$ can be computed. It is found that the assumption of discrete flank contact has only a minor influence on the calculated thermal parameters at the rake face.

Consider now the conditions at the tool–work interface. In Figs 4a, b, c the continuous lines indicate that the magnitudes of ϵ, η, δ (for $\bar{\theta}_{fs}$) are practically independent of $\bar{N}$. It is seen that $\eta/\epsilon \approx 0.2/0.84 = 0.24$. This agrees well with the magnitude of $n/n_2 = 0.26$, as required by equation (30).

Figure 5 gives the $\bar{\theta}_{fs}$–T plot. It is seen that for the entire range of cutting speeds and feeds $T\, \bar{\theta}_{fs}^{\,q'}$ = constant. The value of $q' \approx 5.5$, which is insensitive to $\bar{N}$, can be verified independently using equation (30) for, from this equation, $q' = 1/n\epsilon = 1/(0.22 \times 0.84) = 5.5$ which agrees with the magnitude of q' obtained from Fig. 5.

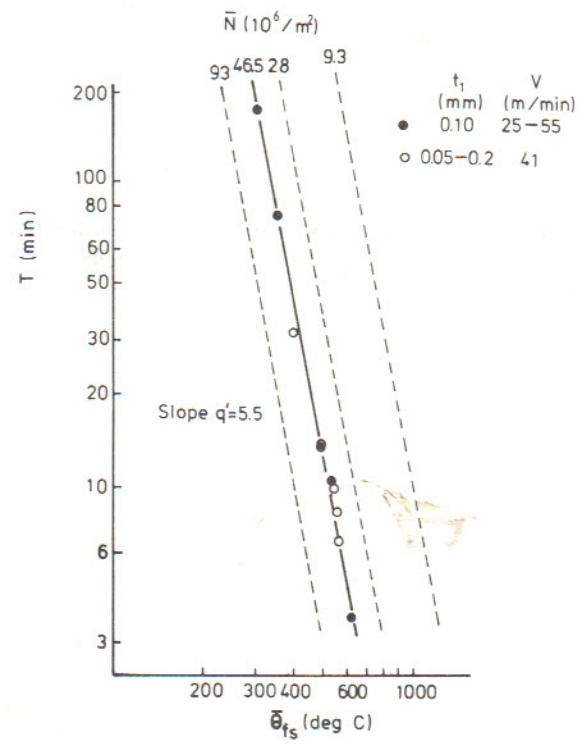

FIG. 5. The relationship between tool life and computed values of $\bar{\theta}_{fs}$ for $V = 25$–55 m/min, $t_1 = 0.05$–0.2 mm and $\ell_f = 0.18$ mm at different values of spot density $\bar{N}$.

The substitution of $q' = 5.5$ in expression (28) gives $0 < \delta < 0.045$. It is interesting to see that $\delta \simeq 0.045$, obtained from Fig. 4c, is close to the upper limit of this range, which suggests that wear at the flank face is of the "layer type" (see Archard [21]).

It is clear from the above discussion that the introduction of the concept of $\bar{\theta}_{fs}$ avoids all the anomalies associated with the use of $\bar{\theta}_f$. However, the exact magnitude of $\bar{\theta}_{fs}$ is still unknown since $\bar{N}$ is unknown but this is not a major disadvantage since the magnitudes of q', ϵ, η and δ, the determination of which constitutes the major practical aim of any cutting temperature analysis, are insensitive to $\bar{N}$. When $\bar{N}$ is changed, the $\bar{\theta}_{fs}$–T line in Fig. 5 merely shifts to another parallel line, so that once the $\bar{\theta}_{fs}$–T curve is plotted empirically, for an arbitrarily chosen N (within a reasonable range), the problem of predicting tool life through temperatures is completely solved (see Fig. 5) since, for any desired set of cutting conditions, we will always calculate $\bar{\theta}_{fs}$ using this *same* arbitrarily chosen value of $\bar{N}$.

Figure 6 shows the relationship between $\bar{N}$ and $\bar{\theta}_{fs}$ for given values of V, t_1, and ℓ_f so that

$$\bar{\theta}_{fs} \approx 43900\, \bar{N}^{-0.4}\, V^{0.84}\, t_1^{0.2}\, \ell_f^{0.045}$$

where V is in m/min and t_1 and ℓ_f are in mm.

It is known, empirically, that cutting tools begin to "burn out" when ℓ_f reaches a critical value $(\ell_f)_{cr}$. Assuming that the critical temperature $(\bar{\theta}_{fs})_{cr}$ is about 600°C for H.S.S. at the onset of burn out, we can obtain an estimate of $\bar{N}$ from equation (32). Substituting the relevant values of V and t_1 and the empirical $(\ell_f)_{cr} = 1.6$ mm, we obtain $\bar{N} = 37.5 \times 10^6$ per m^2. This number, however, can only be taken as a crude indication due to the uncertainties involved in the assumption of $(\bar{\theta}_{fs})_{cr} = 600$°C and in the measurement of $(\ell_f)_{cr}$.

The temperature θ_m measured by the tool–work thermocouple may be estimated, once the temperature distributions at the interfaces are known. This has been done at various cutting speeds (for $\bar{N} = 37.5 \times 10^6$ per m^2), using a procedure similar to that of Lowack

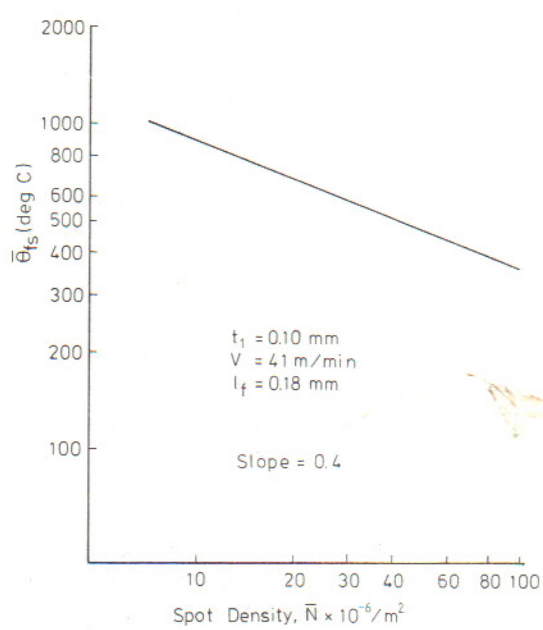

FIG. 6. The relationship between assumed spot density $\bar{N}$ and computed mean flank spot temperature $\bar{\theta}_{fs}$ for $V = 41$ m/min, $t_1 = 0.1$ mm and $\ell_f = 0.18$ mm.

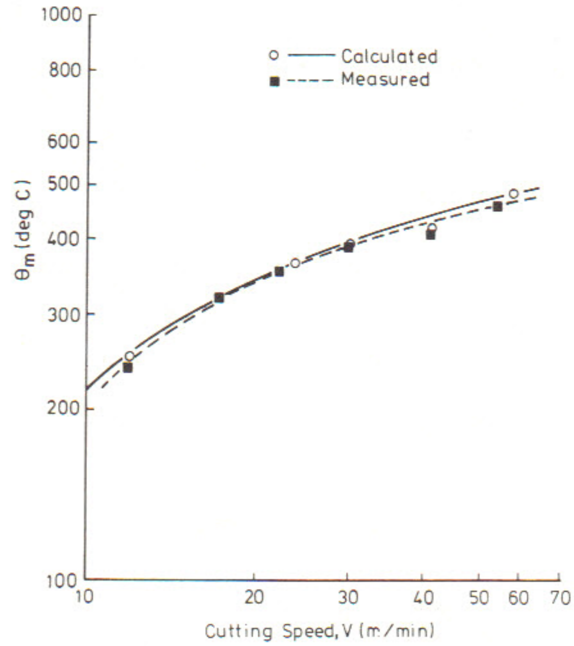

FIG. 7. Comparison of measured tool–work thermocouple temperature θ_m and computed mean flank spot temperature $\bar{\theta}_{fs}$ for $t_1 = 0.1$ mm and $\ell_f = 0.18$ mm and $\bar{N} = 37.5 \times 10^6$ per m^2.

[24] but taking into account the real area of tool–work contact. Figure 7 shows that the estimated and the measured values agree fairly well and a comparison of their magnitudes reveals that θ_m is largely determined by θ_r.

One noteworthy feature of $\bar{\theta}_{fs}$ is that it accounts for the feed-effect (i.e. the magnitude of η) through the work-hardenability of the work material; a factor which can only be identified when the discrete nature of the flank land/workpiece contact is recognised.

CONCLUSIONS

1. The assumption of continuous contact at the tool–work interface, as used in Chao and Trigger's model [7], leads to flank temperatures that are in conflict with empirical evidence on tool wear. The estimated flank temperatures are too low and a minimal effect of feed is predicted.
2. A new parameter, the mean idealised-spot temperature $\bar{\theta}_{fs}$ at tool flank land area, has been developed. This reflects the discrete nature of tool–work contact and the associated thermal constriction resistance.
3. Compatibility between the discrete contact model for flank temperatures and for flank wear can be achieved by assuming that the size of contact spots is determined by the hardness of the workpiece and that the probability of a wear particle being produced, when a tool–work junction is broken, is an increasing function of $\bar{\theta}_{fs}$.
4. The new model for flank temperatures avoids all the anomalies resulting from the continuous flank contact model.
5. While the exact magnitude of $\bar{\theta}_{fs}$ is a function of the assumed spot density, the various indices relating cutting conditions to θ_{fs} are independent of spot density.
6. The index q' in the equation $T\bar{\theta}_{fs}^{q'}$ = constant is insensitive to the assumed spot density. Thus, the problem of relating cutting conditions to tool life through flank temperatures is completely solved once the equation ($T\ \bar{\theta}_{fs}^{q'}$ = constant) is established using an arbitrarily chosen physically reasonable value of the spot density $\bar{N}$. This value of $\bar{N}$ is used in all subsequent calculations of $\bar{\theta}_{fs}$ whenever it is desired to estimate flank temperature for any given set of cutting conditions.

Substituting this value of $\bar{\theta}_{fs}$ into $T\ \bar{\theta}_{fs}^{q'}$ = constant gives us the desired tool life estimate.

7. The insensitivity of q' to cutting conditions and to the value of $\bar{N}$ suggests that it is a fundamental parameter related only to the thermal and physical properties of the tool–work pair.
8. The role of work hardening of work material in determining flank temperatures is more significant than hitherto suspected. An increase in work hardening of the workpiece during the cutting process results in the flank face temperature becoming more strongly dependent on the feed.

Acknowledgements—The authors would like to thank the Director of the Hong Kong Polytechnic for his personal authorization of a research grant and the Directors of Shiu Wing Steel Ltd for their generosity in awarding a matching grant.

REFERENCES

[1] H. S. CARSLAW and J. C. JAEGER, *Introduction to the Mathematical Theory of the Conduction of Heat in Solids*, 2nd Ed., The Clarendon Press, Oxford (1959).
[2] J. C. JAEGER, *Proc. R. Soc. N.S.W.* **76,** 203 (1942).
[3] R. HOLM, *Electric Contacts*, 4th Ed., Springer, Berlin (1967).
[4] R. HOLM, *J. appl. Phys.* **19,** 361 (1948).
[5] C. RUBENSTEIN, *J. Engng Ind.* Ser. B, **98**, 221 (1976).
[6] W. S. LAU, P. K. VENUVINOD and C. RUBENSTEIN, *Int. J. Mach. Tool Des. Res.* **20,** 29 (1980).
[7] B. T. CHAO and K. G. TRIGGER, *Trans. Am. Soc. Mech. Engrs* **80**, 311 (1958).
[8] K. NAKAYAMA, *Bull. Fac. Engng Yokohama* **7**, 1 (1958).
[9] T. N. LOLADZE, *Industrie-Anzeiger* **62,** 991 (1959).
[10] N. N. ZOREV, *Proc. Conf. Technology of Engineering Manufacturing, Inst. Mech. Engrs*, London, 255 (1958).
[11] L. F. KAMSKOV, *Vestn. Mashinostroeniya* **59,** 59 (1959).
[12] H. TAKEYAMA and E. USUI, *Trans. Am. Soc. Mech. Engrs* **80**, 1089 (1959).
[13] P. W. WALLACE and G. BOOTHROYD, *J. Mech. Eng. Sci.* **6,** 74 (1964).
[14] E. G. LOEWEN and M. C. SHAW, *Trans. Am. Soc. Mech. Engrs* **76**, 217 (1954).
[15] P. D. MURARKA, G. BARROW and S. HINDUJA, *Int. J. Mech. Sci.* **21,** 445 (1979).
[16] P. K. WRIGHT, S. P. MCCORMICK and T. R. MILLER, *J. Engng Ind.* Ser. B, **102**, 123 (1980).
[17] R. CONNOLLY and C. RUBENSTEIN, *Int. J. Mech. Tool Des. Res.* **8,** 159 (1968).
[18] W. S. LAU and C. RUBENSTEIN, *Int. J. Mach. Tool Des. Res.* **12,** 311 (1972).
[19] S. KOBAYASHI and E. G. THOMSEN, *J. Engng Ind.* Ser. B, **82**, 324 (1960).
[20] F. P. BOWDEN and D. TABOR, *The Friction and Lubrication of Solids*, Part I (1971 Impression), Oxford University Press, London (1950).
[21] J. F. ARCHARD, *J. appl. Phys.* **24,** 981 (1953).
[22] H. SCHALLBROCH and H. SCHAUMANN, *VDI Z.* **81,** 325 (1937).
[23] J. T. BURWELL and C. D. STRANG, *J. appl. Phys.* **23,** 18 (1952).
[24] H. LOWACK, Dr Ing. Dissertation, der Rheinisch–Westfalischer Technischer Hochschule, Aachen (January 1967).